Materials Research, Vol. 8, No. 4, 395-400, 2005

Nanocrystalline Material in Toroidal Cores for Current Transformer: Analytical Study and Computational Simulations

Benedito Antonio Luciano[a]*, *João Marcelo Cavalcante de Albuquerque*[a], *Walman Benício de Castro*[b], *Conrado Ramos Moreira Afonso*[c]

[a]*Department of Electrical Engineering, CEEI/UFCG, P. B. 10105, 58109 970 Campina Grande - PB, Brazil*
[b]*Department of Mechanical Engineering, CCT/UFCG, 58109-970 Campina Grande - PB, Brazil*
[c]*Materials Engineering, Pos-Graduate Program in Materials Science Engineering, UFSCar, Via Washington Luís, km 235, 13565-905 São Carlos - SP, Brazil*

Received: July 19, 2004; Revised: October 19, 2005

Based on electrical and magnetic properties, such as saturation magnetization, initial permeability, and coercivity, in this work are presented some considerations about the possibilities of applications of nanocrystalline alloys in toroidal cores for current transformers. It is discussed how the magnetic characteristics of the core material affect the performance of the current transformer. From the magnetic characterization and the computational simulations, using the finite element method (FEM), it has been verified that, at the typical CT operation value of flux density, the nanocrystalline alloys properties reinforce the hypothesis that the use of these materials in measurement CT cores can reduce the ratio and phase errors and can also improve its accuracy class.

Keywords: *nanocrystalline alloys, toroidal cores, current transformer*

1. Introduction

Current transformer (CT) is an instrument transformer specially designed and assembled to be used in measurement, control, and protective circuits. Its primary circuit consists of a few turns – sometimes even a single turn – and is connected in serie with the circuit whose current is desired to be measured, and the secondary circuit is connected to the current-measuring instruments.

The theory about CT is basically the same of any other iron-core transformer. The secondary circuit is closed through the typical low impedance of the instruments connected to it. Normally, these are 5 A instruments. The voltage across the secondary terminals is the drop through the instruments and loads, and usually is only a few volts. The voltage across the primary terminals is approximately the voltage referred to the primary, and can be only a fraction of a volt.

In the ideal CT, the secondary current is inversely proportional to the ratio of turns and oppositive in phase to the impressed primary current. However, an exact inverse proportionality and phase relation are not possible because part of the primary current must be used to excite the magnetic material of the core. So, the exciting current must be subtracted phasorially from the primary current to find the amount remaining to supply secondary current. This value will be slightly different from the value that the ratio of turns would indicate and there is a slight shift in the phase relationship. This results in the introduction of ratio and phase angle errors when compared to the ideal CT.

Since the exciting current alters the ratio and phase angle of the primary and secondary currents, it is made as small as possible through the use of high permeability and low loss magnetic materials in the construction of the core, such as silicon steel and amorphous alloys. In many industrial applications, designers need to select the magnetic core material and its shape. Each specific application demands the development of a specific core shape. Therefore, they all have advantages and drawback; for instance, toroidal cores are more compact than E-cores and their material cost is lower due to single component and tighter magnetic coupling[1].

In this work, it is presented a study about the possibilities of application of nanocrystalline alloys in toroidal cores for current transformers.

2. Analytical Study and Some Design Considerations

Current transformers are characterized by some relationships. The first is the marked ratio of the primary current to the secondary current ($K_c = I_{pn} / I_{sn}$), and is indicated by the manufacturer. This ratio is a fixed and permanent value for a given current transformer. The second is the true ratio of the rms primary current to the rms secondary current ($K_r = I_p / I_s$) under specified conditions. The true ratio of a current transformer is not a single fixed value, since it depends on the specified conditions of use, such as secondary burden (Z_c), primary current (I_p), frequency (f), and wave form. The third is the ratio correction factor (RCF). It is the factor by which the marked ratio must be multiplied to obtain the true ratio (RCF = K_r / K_c).

The CT errors exist due to the exciting current I_e at the magnetizing branch Z_m. The primary impedance do not affects the CT errors and it is represented by a low-impedance in serie with the system circuit where the CT is installed, which value can be neglected. After

*e-mail: benedito@dee.ufcg.edu.br

these considerations, Figure 1 can represent the CT electrical model, where Z_s is the secondary impedance.

2.1. Phase angle

The phase angle of a current transformer, designated by the Greek letter β, is the angle between the current leaving the identified secondary terminal and the current entering the identified primary terminal, under specified conditions[2]. It is apparent from Figure 2 that the reversed secondary current I_2 is not in phase with the impressed primary current I_1, there is an angle between them, the phase angle β. This angle is considered positive when the secondary current leads the primary current and it is usually expressed in minutes.

In this Figure, ϕ is the magnetizing flux and I_0 is the exciting current with its two components: I_μ, the magnetizing current, and I_p, the active losses current. In the secondary circuit: E_2 is the induced electromotive force, r_2 is the winding resistance, x_2 is the leakage reactance, U_2 is the terminal voltage, I_2 is the secondary current, and θ_2 is the angle between U_2 and I_2. In addition, it can be seen that the primary current I_1 is obtained by phasor sum of I_0 and $(-n_2/n_1)$. I_2, where n_2 and n_1 are the number of turns of the secondary and primary windings, respectively.

2.2. The influence of the primary and the secondary currents on the CT errors

The ratio error ε_c is defined as the percent relative difference between the measured value of the primary current and its exact value, as expressed by the equation:

$$\varepsilon_c = \frac{K_r.I_2 - |\vec{I}_1|}{|\vec{I}_1|}.100\% \quad (1)$$

On the other hand, the phase angle error is defined as the angle β presented on the phasor diagram of the CT in Figure 2.

The main reason for the ratio and phase angle errors of a current transformer is the exciting current I_0. In an ideal TC, in which I_0 does not exist, $\vec{I}_1$ and $-(n_2/n_1)$. $\vec{I}_2$ presented in Figure 2 are coincident. Thus, the primary current value, obtained from the secondary current, would be equal to the absolute value of the vector $\vec{I}_1$ from the phasor diagram, and this vector would be delayed from $\vec{I}_2$ of exactly 180°.

In conventional transformers, the exciting current is considered constant, and its absolute value and phase can be determined by open-circuit test. However, this is not true in CT. In a current transformer the exciting current is not constant, neither in its absolute value nor in its phase, due to the great influence of the non-linearity of the magnetic material of which its core is made. Due to the relation between the primary and the exciting currents, the smaller the value of the first one, the greater the influence of the second, what increases the ratio and phase angle errors of the CT. That is why, when determining the accuracy class of a CT, the technical norms allow the CT to present bigger errors when tested with 10% of the primary nominal current than when it is tested with its exact value.

Analysing Figure 2, it can be verified the influence of the exciting and the primary currents on the errors of a CT. In this figure, projecting the vectors $\vec{I}_o$ and $\vec{I}_2$ over the vector $\vec{I}_1$, it is obtained:

$$|\vec{I}_1| = K_c.|\vec{I}_2|.\cos\beta + |\vec{I}_o|.\cos\left[90° - (\alpha + \beta + \delta)\right] \quad (2)$$

where α is the angle between the exciting current $\vec{I}_o$ and the magnetizing flux $\vec{\phi}$, and δ is the angle between the inverse of $\vec{I}_2$ and the inverse of $\vec{E}_2$.

Due to its relatively small value, the angle β can be neglected, simplifying the previous expression:

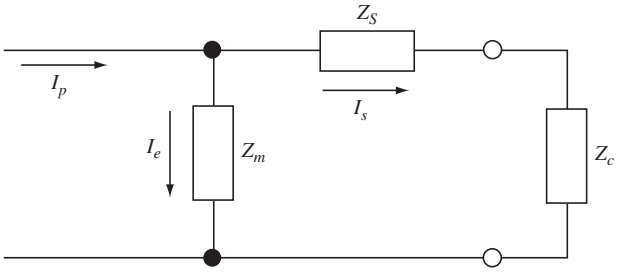

Figure 1. Equivalent electric circuit of a current transformer.

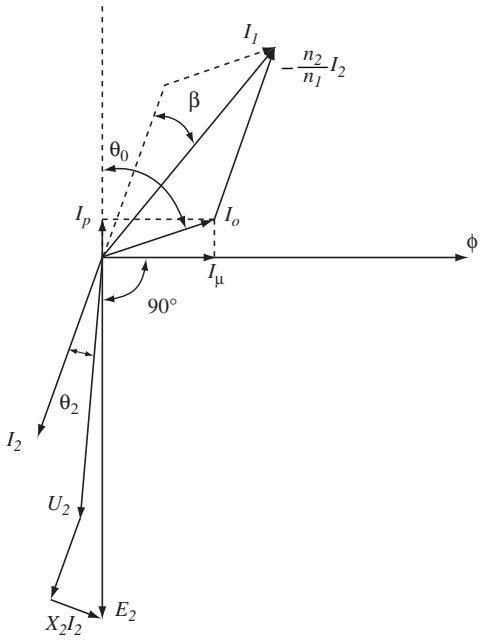

Figure 2. Phasor diagram of a current transformer.

$$|\vec{I}_1| = K_c.|\vec{I}_2| + |\vec{I}_o|.\operatorname{sen}(\alpha + \beta) \Rightarrow \quad (3)$$

$$\frac{K_c|\vec{I}_2| - |\vec{I}_1|}{|\vec{I}_1|} = -\frac{|\vec{I}_o|}{|\vec{I}_1|}.\operatorname{sen}(\alpha + \delta)$$

Analysing the second equality of expression (3), it can be seen that its first member is equal to the ratio error of the CT, which will be considered in its absolute value in a new expression:

$$\frac{K_c.|\vec{I}_2| - |\vec{I}_1|}{|\vec{I}_1|} = -\frac{|\vec{I}_o|}{|\vec{I}_1|}.\operatorname{sen}(\alpha + \delta) \Rightarrow \varepsilon_c = \frac{I_o}{I_1}.\operatorname{sen}(\alpha + \delta) \quad (4)$$

Again from the phasor diagram of Figure 2, the follow expression for the tangent of the angle β can be obtained:

$$tg\beta = \frac{|\vec{I}_o|.\operatorname{sen}\left[90° - (\alpha + \beta + \delta)\right]}{K_c.|\vec{I}_2|.\cos\beta} \quad (5)$$

Considering that the angle β has a relatively small value, a simpler expression can be, then, obtained:

$$\beta = \frac{|\vec{I}_o|}{|\vec{I}_1|}.\cos(\alpha + \delta) \quad (6)$$

As verified in Equations 4 and 6, both the ratio and phase angle errors of the CT increase as the exciting current increases or the

primary current decreases. Then, it is important that the magnetic material of the CT core could demand a small exciting current to be magnetized and, also, that the CT could be projected to operate with a primary current value as near as possible of its nominal value, in order to minimize the effects of the primary current in its errors.

In turn, the secondary current of a CT is extremely dependent of its primary current, and it is not influenced by the impedance of the element connected to the secondary terminals of the CT. However, if this impedance exceeds some limit values, determined by the maximum power with which the accuracy class of the CT was obtained, the errors can be much greater than those obtained with the tests.

When an impedance Z is connected to the secondary of a CT, a current I_2 flows through it and the ratio and phase angle errors ε_c and β, respectively, can be determined by Equations 4 and 6. When the absolute value of Z increases, keeping its phase unchanged, it is necessary an increase of the secondary voltage U_2 so that the secondary current I_2 could stay constant. To achieve this aim, the electromotive force E_2 has to increase its absolute value and so on the flux φ inside the core. As this flux is produced by the exciting current I_o, it must also increase its absolute value, increasing the ratio and phase angle errors. This analysis of the influence of the secondary current on the CT errors is important, because it alerts about the resistance limit of the conductors that could be used to connect the secondary windings of the CT to the equipments that they will supply.

2.3. Some design considerations

An essential part of the transformer design consists of the determination of the magnetic cross-section area (A_{mag}) and the conductors cross-section area. These areas are determined from estimations of suitable values for the peak flux density B_m; the full-load rms current density J in the windings, that depends on the way transformers will be used, intermittently or continuously; the winding space factor k_w; and the stacking factor k_s.

The primary and secondary windings must be accommodated in the window area A_w. The winding space factor k_w is defined as the ratio between the total conductor cross-section area and the window area. Insulation and clearance reduce the available area for actual conductor cross-section to $k_w.A_w$. The full-load rms current density in the windings J is limited by $r.I^2$ loss and heat dissipation. The stacking factor k_s is defined as the ratio between the magnetic cross-section area and the total core cross-section area.

As nanocrystalline materials are produced in the form of ribbons, it is available toroidal cores with square or rectangular cross-section, as shown in Figure 3.

The dimensioning of the magnetic circuit starts with the determination of the magnetic cross-section area, given by:

$$A_{mag} = k_s.A_{geo} \tag{7}$$

where A_{geo} is the geometric cross-section area.

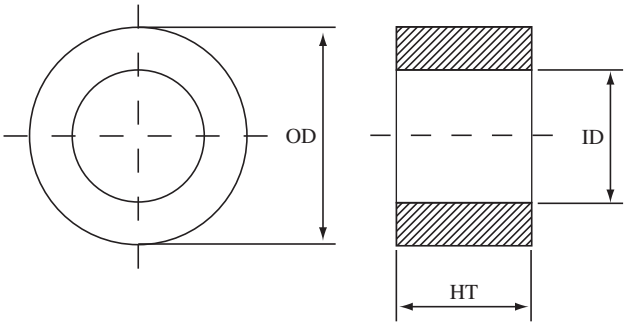

OD = Outer diameter ID = Inner diameter HT = Height

Figure 3. Toroidal core geometry.

The medium length of the magnetic circuit is given by:

$$l_{mag} = \pi\left(\frac{OD + ID}{2}\right) \tag{8}$$

The number of each winding turns N is obtained by the equation:

$$N = \frac{V}{k_f.f.B_m.A_{mag}} \tag{9}$$

where V is the rated rms voltage, f is the frequency of the signals, and k_f is the form factor (equal to 4.44 for sine wave and equal to 4.0 for square wave).

The cross-section areas of the two windings, the primary (A_p) and secondary (A_s), are determined considering the full-load rms current density in the winding and the work rate of the transformer, by the following relationships:

$$A_p = \frac{S}{J.V_1} \tag{10}$$

$$A_s = \frac{S}{J.V_2} \tag{11}$$

Because of the m.m.f. balance ($N_1.I_1 = N_2.I_2$), each one of the primary and secondary windings occupy about one-half of the available area, so that the primary current linkage is $N_1.I_1 = (1/2).k_w.A_w.J$ and the rms value of the current is given by:

$$I_{rms} = \frac{k_w.A_w.J}{2.N} \tag{12}$$

where A_w is the geometrical core window area and k_w is the winding factor.

By Faraday's law, for sinusoidal wave, the rms value of the voltage is:

$$V_{rms} = 4.44.f.N.A_{mag}.B_m \tag{13}$$

Therefore, as $V_{rms} = S/I_{rms}$, the transformer volt-ampere rating is given by:

$$S = 2.22.f.B_m.J.K_w.A_w.A_{mag} \tag{14}$$

It is shown in Equation 14 that the transformer volt-ampere rating is proportional to the product of the available window area of the core multiplied by the magnetic cross-section area, which is called area product. There is a unique relationship between this area product, characteristic value for transformer cores, and several other important parameters that must be considered in transformers design, such as volume, weight, surface area and current density, for a given temperature rise[3].

Using Ampère's law, and considering the total m.m.f. for a peak flux density as $H_m l_{mag}$, where l_{mag} is the mean length of the flux path around the magnetic circuit, the magnetizing current I_m in the N_1 turns of the primary windings, ignoring harmonics, is given by:

$$I_m = \frac{H_m.l_{mag}}{\sqrt{2}.N_1} \tag{15}$$

3. Nanocrystaline Alloys Development

The first nanocomposite soft magnetic alloy based on the Fe-Cu-M(-Si)-B alloy (M: Nb, Mo, Ta, W, Zr, etc.) was obtained by Yoshizawa et al.[4]. The first step was to produce amorphous metal ribbons of about 20 μm thickness. Next, the amorphous ribbons were wound into toroidal cores, and then the core materials were annealed to produce the nanocrystalline soft magnetic material with an average grain size of approximately 10 nm[5].

After Yoshizawa et al. report[4], nanocrystalline materials have been investigated for applications in magnetic devices requiring

both magnetically hard and soft materials. In particular, amorphous and nanocrystalline alloys have been used as the core material in some electromagnetic devices, such as distribution transformers, common mode choke coils, pulse transformers, impulse current transformers, transformers for switched-mode power supplies and current transformers[6].

4. Magnetic Characterization

In Figures 4, 5 and 6 are presented the hysteresis curve at 60 Hz, the permeability curve at 60 Hz and the initial magnetization curve at 5 Hz, obtained for the nanocrystalline alloy FINEMET® FT-3M F6045G produced by Hitachi Metals Ltd.

From the magnetic characterization, it has been verified that, to the typical CT operation value of 0.2 T, the nanocrystalline properties reinforce the hypothesis that the use of these materials in measurement CT cores can reduce both the relation and phase errors and can also improve its accuracy class.

5. Numerical Calculation Using FEMM Package

Whilst analytical method is useful for must problems concerning transformers design, the numerical methods provide a better understanding of transformers electromagnetic behavior. Indeed, numerical methods, such as the finite element method, allow an accurate determination of flux densities in the whole domain and also the study of local phenomena. In this work, a finite element method computer program was carried out in order to obtain the flux density inside the magnetic material in the toroidal core CT previously designed. These simulations were performed using the electromagnetic package FEMM 3.3 applied for low frequencies[7].

In the simulations, a quarter of the toroidal core was chosen as the domain of study, as this part of the entire geometry presents symmetry along the horizontal and vertical axies. This proceeding helps to reduce the processing time needed. The program FEMM 3.3 was used to simulate the behaviour of a CT whose electrical and magnetic circuits were previously designed by analytical proceedings. Four simulations were realized, which aimed to compare the CT performance when its core was composed of four different magnetic materials.

The magnetic materials chosen to be compared as the CT core material were: the nanocrystalline alloy FINEMET® FT-3M F6045G, produced by the Japanese company Hitachi Metals Ltd.; the amorphous alloy METGLAS® 2605S-2, produced by the American company Honeywell International; the nanocrystalline alloy NANOPERM® M-033-03 N1, produced by the German company Magnetec GmbH; and grain oriented (GO) silicon-iron E-004, produced by the Brasilian company Acesita.

In Table 1 there are some magnetic characteristics of the magnetic materials studied in the simulations. Silicon steel is an example of magnetic material commonly used in the cores of commercial CT. Thus, the simulations could compare the performance between ferrocrystalline conventional materials and new magnetic materials as CT cores. In this table, B_s is the saturation flux density, μ_{rmax} is the maximum value of the relative permeability, and ρ is the resistivity of the material.

A CT is used in such a way that the magnitude of secondary current has negligible influence on magnitude of the primary current. Thus, as the primary winding gives the necessary energy to the core magnetization, it was the only one winding designed in simulations. Its eight turns were uniformly distributed along the core and just two of then appear in the quarter designed. The conductor used in the primary winding is made of copper and, according to the previous calculations, has the diameter of the wire 5 AWG. To design the core, it was used the real dimensions of the magnetic material and of the

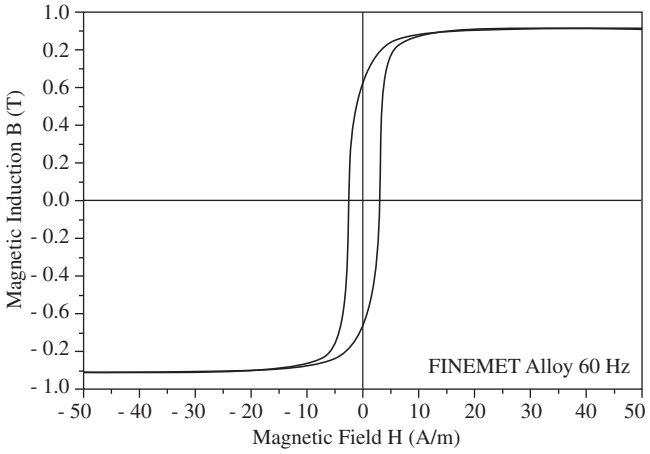

Figure 4. Hysteresis curve at 60 Hz.

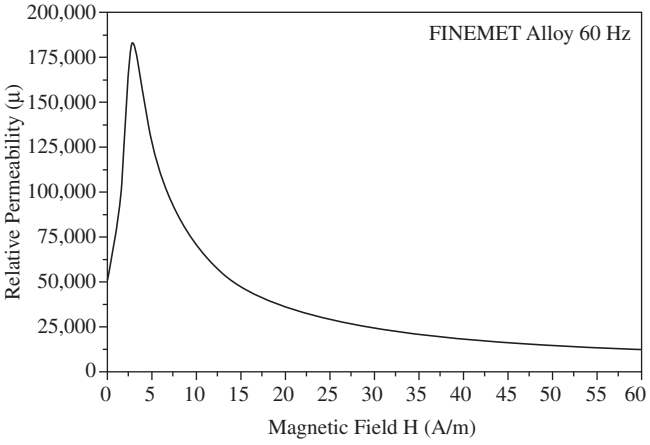

Figure 5. Magnetic permeability curve at 60 Hz.

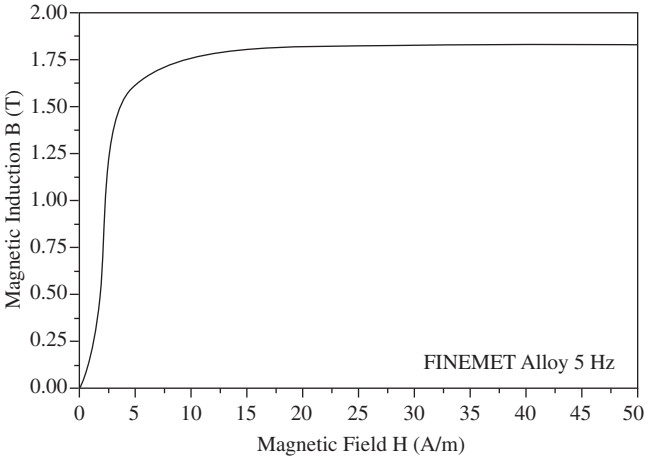

Figure 6. Initial magnetization curve at 5 Hz.

capsule of non-magnetic material that envolves the core FINEMET® FT-3M F6045G. The domain of study divided in the finite elements of the mesh is shown in Figure 7.

To analyse the performance of the CT, the dimensions and the constitutive parts of the problem were always kept the same in every simulation, just changing the characteristics of the magnetic

material that would occupy the place in the domain reserved to the core. From the resuts given by the program, some informations were collected for each one of the magnetic materials studied. These data were: the magnetic field intensity (H) in the place of the core where the magnetic induction reached the desired value of 0.2 T; the relative magnetic permeability (μ_R) at this point; and the excitation current (I_o) necessary to obtain that operation induction value. In Table 2 can be seen these values obtained for every magnetic material studied.

In Figure 8 is shown one of the graphics provided by FEMM 3.3 for the simulation using the nanocrystalline alloy FINEMET® FT-3M F6045G. The magnetic flux lines stay confined within the magnetic material of the core, due to its high relative permeability value in comparison with the others elements of the domain. The intensity of the magnetic flux can be observed by the colour scale in the figure, where the more intense is the red tinge, the greater is the flux density in the material.

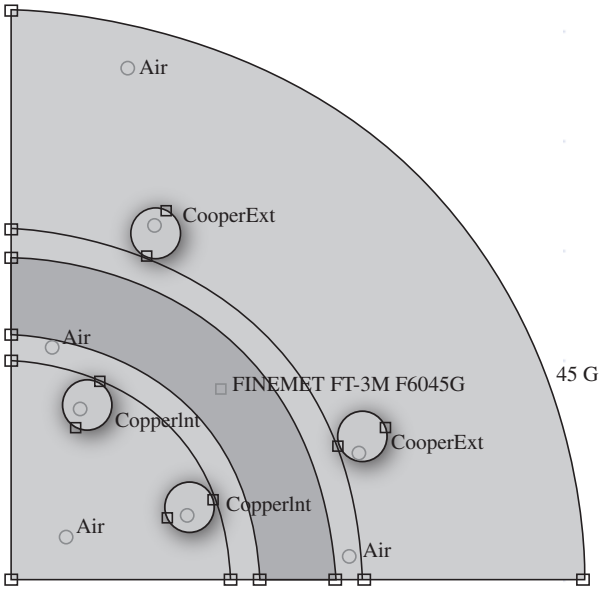

Figure 7. Domain divided in the elements of the mesh.

The calculations show that the field and flux density vary radially in a wound toroid. In each simulation, the copper turns of the primary winding conducted the calculated value of exciting current necessary to induce inside each magnetic material a mean flux density of 0.2 T. To reach this particular value of magnetic induction in the core, the nanocrystalline alloy FINEMET® FT-3M F6045G was the magnetic material that demanded the lowest value of exciting current, followed by the amorphous alloy METGLAS® 2605S-2. Their values of exciting currents are extremely lower than the one demanded by the GO silicon-iron E-004, which does not present a high magnetic permeability at the CT operation induction value. Finally, the other nanocrystalline alloy, NANOPERM® M-033-03 N1, although presenting very low rates of magnetic losses at 60 Hz, also needed a relatively high value of exciting current. This alloy congregates good magnetic properties in general, but particularly at 0.2 T your relative magnetic permeability is very lower than that presented by the nanocrystalline alloy FINEMET® FT-3M F6045G.

6. Conclusions

From the magnetic characterization and the computational simulations, using the finite element method (FEM), it has been verified that, at the typical current transformers operation value of 0.2 T, the nanocrystalline alloys properties reinforce the hypothesis that the use of these materials in measurement current transformer cores can reduce the relation and phase errors and can also improve its accuracy class.

Acknowledgments

The authors are grateful to Hitachi Metals Ltd. and Magnetec GmbH for providing the nanocrystalline alloys in toroidal cores shape, and to ACESITA and TOROID for the important informations conceded. The present investigation was sponsored by PROCAD/CAPES – 0104/01-9 and CNPq.

Table 1. Magnetic materials simulated as CT cores.

Material	Composition	B_s (T) (60 Hz)	μ_{rmax} (60 Hz)	ρ (μΩ.m)
FINEMET® FT-3M F6045G	$Fe_{73,5}Cu_1Nb_3Si_{13,5}B_9$	0.90	185,000 (3.0 A.m^{-1})	1.20
NANOPERM® M-033-03 N1	$Fe_{73,5}Si_{15,5}Cu_1Nb_3B_7$	1.18	34,985 (1.8 A.m^{-1})	1.15
METGLAS® 2605S-2	$Fe_{78}Si_9B_{13}$	1.56	193,397 (4.3 A.m^{-1})	1.37
Silicon-iron GO E-004	Fe-3.2%Si	1.85	40,154 (23.0 A.m^{-1})	0.47

Table 2. Parameters obtained for each magnetic material by simulation.

Magnetic Material	Values Obtained by Simulation for 0.2 T and 60 Hz		
	H (A.m^{-1})	μ_R	I_o (mA)
FINEMET® FT-3M F6045G	1.46	109,100	31.34
NANOPERM® M-033-03 N1	5.43	29,270	110.70
METGLAS® 2605S-2	1.64	97,090	34.82
Silicon-iron GO E-004	6.93	22,930	141.36

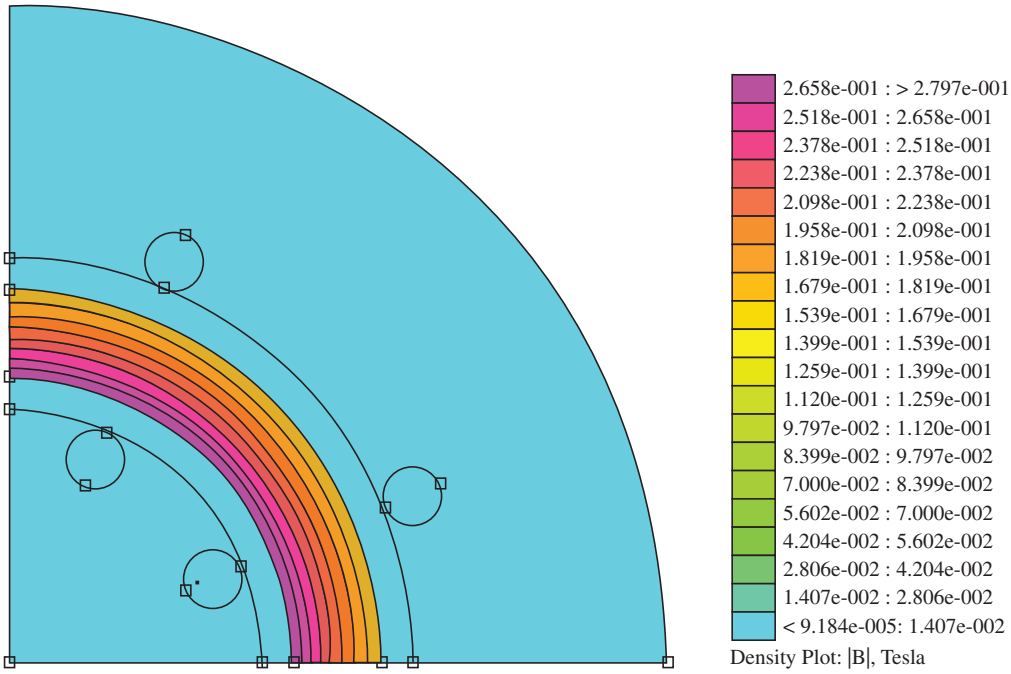

Figure 8. Scale of flux density in the elements of the domain.

References

1. Luciano BA, Guimarães MKA, Castro WB. Journal of metastable and nanocrystalline materials. In: Kiminami, CK, Botta Filho WJ, guest editors. *Some designs considerations on industrial applications of amorphous and nanocrystalline alloys. Proceedings of the 1st Workshop on Metastable and Nanostrutured Materials*; 2001 August 16-17; *São Pedro, SP, Brazil*. Switzerland: Trans Tech Publications. 2002. p. 133-138.
2. Edison Electric Institute. *Electrical Metermen´s Handbook*. Seventh Edition. New York: EEI: 1965.
3. McLyman, CWT. *Magnetic core selection for transformers and inductors: a user's guide to practice and specification*. New York: Marcel Dekker: 1997.
4. Yoshizawa Y, Oguma S, Yamauchi K. New Fe-based soft magnetic alloys composed of ultrafine grain structure. *Journal of Applied Physics*. 1988; 64(1):6044-6046.
5. Yoshizawa Y. Magnetic properties and microstructure of nanocrystalline Fe-based alloys. *Journal Metastable and Nanocrystalline Materials*. 1999; 1(1):51-62.
6. Mchenry ME, Laughlin DE. Nano-scale materials development for future magnetic applications. *Acta Materialia*. 2000; 48(1):223-238.
7. Meeker D. *Finite Element Method Magnetics – Version 3.3*. [user's manual on the Internet]. 2003. [cited 2003 May 17] Available from: http://femm.berlios.de.